High biomass density promotes density-dependent microbial growth rate

Emna Krichen, Jérôme Harmand, Michel Torrijos, Jean-Jacques Godon, Nicolas Bernet, Alain Rapaport

High biomass density promotes density-dependent microbial growth rate

E. Krichen[a,c,d,*], J. Harmand[b], M. Torrijos[b], J. J. Godon[b], N. Bernet[b], A. Rapaport[c]

[a] U. Montpellier, LabexNumev, 34095 Montpellier, France

[b] LBE, INRA, Univ Montpellier, 11100 Narbonne, France

[c] MISTEA, INRA, Montpellier Supagro, Univ Montpellier, 34060 Montpellier, France

[d] UMR CNRS, IRD, Ifremer, U. Montpellier MARBEC, 34203 Sète, France

[*] Corresponding author. Email address: emna.krichen@supagro.inra.fr

ABSTRACT

Describing the interactions between a population and its resources is a research topic in both microbiology and population ecology. When there are fewer resources for the individuals in a large population, the overcrowding can lead to a density-dependent effect which is reflected by a negative feedback of' the organism density on the consumption process. In this paper, we investigate the growth rate of an aerobic microbial ecosystem by two series of experiments performed in continuous agitated cultures. Using a constant dilution rate, but different input substrate concentrations in each experiment, the biomass and substrate concentration were measured at steady state to confront their values with those obtained theoretically from the well-known mathematical model of the chemostat using either resource or density-dependent kinetics. The structures of both flocs and microbial communities were monitored in order to interpret the results. The experiments confirm that density-dependent growth-rate can result either from a high concentration of biomass or from the structuration of this biomass into flocs and we have shown that a new parametrized family of growth functions, that we proposed in this paper, suits better the experimental data than Monod or Contois growth functions.

Keywords

Density-dependent growth rate, microbial ecosystem, mass balance models, flocculation, microbial ecosystem structure

Nomenclature

μ_{max} maximum specific growth rate, (/day)
CSTR Continuous Stirred Tank Reactor
D dilution rate, (/day)
COD chemical oxygen demand, (gO_2L^{-1})
FSD floc size distribution
HRT hydraulic residence time, (day)
J mean square criterion
K_s half-saturation constant, (g/L)
PCR Polymerase Chain Reaction

Q_{in} input flow rate, (l/day)
Q_{out} output flow rate, (l/day)
RPM rotation per minute
s^* substrate concentration at steady state, (g/L)
SE1 first series
SE2 second series
S_{in} input substrate concentration, (g/L)
SS suspended solids, (g/L)
SSCP Single Strand Conformation Polymorphism
V reactor volume, (L)
x^* biomass concentration at steady state, (g/L)
Y Yield, (%)

1. INTRODUCTION

The study of predator-prey interactions has been the object of intense researches for several years. As in many subfields of ecology, the science behind predator-prey investigations has been driven by theory, including important advances in mathematical models as tools for understanding and predicting the functioning of ecosystems (*cf.* Wade et *al.*, 2016). Predator-prey models have been studied mathematically since the publication of the Lotka-Volterra equations in 1920 and 1926 based on the hypothesis of resource (prey)-dependence where the functional response of the predator (*i.e.* number of prey captured per predator per unit of time) is a function of the absolute prey density noted g(N). This hypothesis was questioned by R. Aridity and L. Ginzburg in the 1990s (see Arditi and Ginzburg, 1990 or their recent book on density-dependence, Aridity and Ginzburg, 2012), who proposed a specific case of density-dependence, named ratio-dependence, where the prey capture rate is a function of the ratio of the prey density over predator density noted g(N/P).

In microbiology, researchers have often faced similar problems in describing the growth-rate of microorganisms growing on substrates or in the study of competition through resource depletion. The modelling of the functional response, also named the microbial specific growth rate or the reaction kinetics was lifted at the same time in theoretical ecology and in microbial ecology. It is particularly interesting to notice that several models, developed in these two disciplines independently, and thus bearing different names, propose in fact the same growth rate expressions (Jost, 2000). In other words, the same mathematical functions are used to describe micro as well as macro-organisms growth. The latter being more difficult to handle than microbes, the microbiology has appeared since a few years as a field, particularly suited to study questions of general ecology (Jessup and Kassen, 2004). If we exclude complex mechanisms such as inhibition, functions describing the growth rate of microorganisms can be classified into two main classes, depending whether they involve only the resource (substrate or nutrient) concentration in the medium containing the culture, as in the case of the Monod model (Monod, 1950) or both substrate and biomass (or predator) densities as in the case

of the Contois model (Contois, 1959). In fact, what is of relative importance with respect to a pure culture (both models have very similar predictions for pure cultures) becomes very important for complex ecosystems in the sense Monod-like models predict extinction of all species in competition on a single substrate, but one (this well-known property is called the competitive exclusion principle and has been studied in ecology from the 1950s, *cf.* for instance Hardin, 1960) while Contois-like models allow coexistence of several species (*cf.* for instance Lobry and Harmand, 2006).

If we consider Monod functions, for a constant feed rate, the chemostat theory predicts that the equilibrium should only depend on the dilution rate D and be independent of the input substrate concentration S_{in} (on the condition that this latter one is large enough to supply enough resource for the micro-organisms to grow). This prediction was tested by varying dilution rates and influent substrate concentration and letting the chemostat reaching its steady state while measuring the effluent substrate concentration s^* (Jost, 2000). However, it was only verified for pure cultures. When working with mixed cultures (such as in wastewater treatment or fermentation processes) or using a multicomponent substrate, it is well known that the effluent concentration do not depend only on the dilution rate, but also on the concentration of substrate S_{in} in the influent (Grady et *al.* 1972, Grady and Williams 1975, Elmaleh and Ben Aim 1976, Daigger and Grady 1977). The independence of the growth rate at steady state with respect to S_{in} in the chemostat has been questioned, following experimental observations since 1959 by Contois, Yoshinori (1963) by including the ratio s/x in the expression of the growth rate instead of the absolute value of available substrate and thus emerging an effect of density-dependence. On the latter, the question of the mechanisms at the origin of this phenomenon can be questioned.

In the present work, we investigate whether a high density of biomass can generate density-dependent growth rate as proposed in Harmand and Godon (2007), and formalized in Lobry and Harmand, (2006). We therefore propose experiments in a chemostat or *CSTR* (Continuous Stirred Tank Reactor) followed by a macroscopic modelling approach and a study of the proposed models to determine what type of growth rate is the most appropriate to explain the experimental data. The novelty with respect to the literature lies in the fact we have followed not only substrate and biomass densities but also monitored microbiology of the complex ecosystem used together with the structure of the biomass. Our results show that density-dependent kinetics may emerge not only from a high density, but also from the structuration of the biomass in flocs.

The paper is organized as follows. We first describe the experiments we performed in chemostat with the different parameters we monitored, we recall the qualitative predictions that can be done from the assumptions on the microbial growth rate at the scale of the whole biomass and we describe the method of the models identification. Then, we show and analyse the results at the light of the

monitored parameters and of the modelling approach before some conclusions and perspectives are drawn.

2. MATERIAL AND METHODS

2.1. Experimental setup and experiment

The experimental work is divided into two consecutive series of experiments applied in a chemostat device: a first series, named SE1, with increasing substrate step-loads and a second series SE2 where these loads were applied decreasingly. A hydraulic retention time of 24 h was maintained constant throughout the experiments.

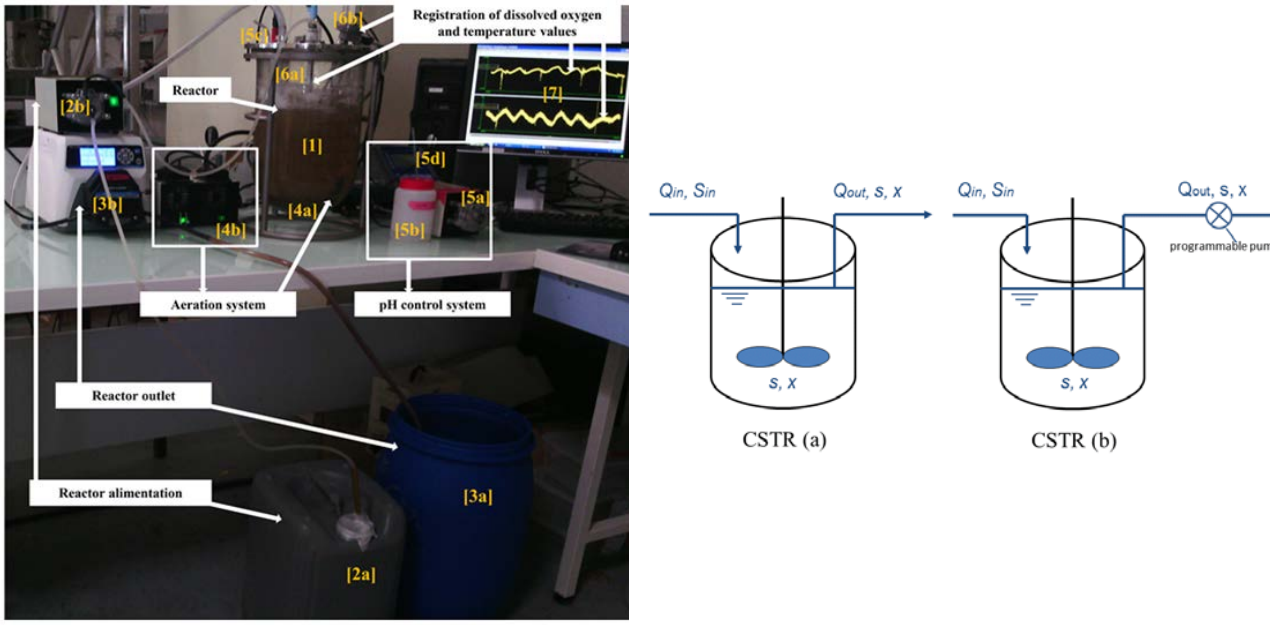

Figure1: Experimental setup

All experiments were carried out in the same continuous biological reactor (Fig. 1). The reactor consisted of a glass vessel (noted [1] on Figure 1) inoculated with constant total volume of 6.8 L of biomass *x* obtained from a return sludge pump of the activated sludge of the treatment plant of Narbonne (handling approximately 60000 EH). The substrate *s* used to feed the reactor is red wine (Bag-In-Box of 5L, Winery: Club des Sommeliers, Grapes: Cabernet Sauvignon, Wine Region: Pays d'Oc, France) whose initial pH (potential of hydrogen) and COD_t (total chemical oxygen demand) are 3.82 and 250.3 $gO2L^{-1}$ respectively. The choice of this substrate is based on the fact that wine is a highly biodegradable substrate. The input substrate concentration S_{in} is daily prepared (7 L), stored in a feed tank [2a] except during weekends where it is stored in a larger tank of 21 L. The reactor was fed continuously and the S_{in} step changes were done by diluting the red wine with water. The *COD/N/P* ratio was adjusted with $NH_4H_2PO_4$ and NH_4Cl in order to equal 200/5/1. The organic loading rate was changed each time the equilibrium was established for a given concentration S_{in}.

The substrate was introduced into the glass vessel by a 16mm diameter pipe and a pump (5 RPM, type Master flex) [2b] with an input flow rate Q_{in} = 4.6 ml/min. Moreover, the excess of bioreactor liquid was collected in a can [3a], using another pump Q_{out} [3b]. During experiments *SE1*, a continuous pump was used to maintain the useful volume *V* constant in the reactor, which implied Q_{out} to equal the input flow rate (*CSTR (a)* Fig. 1). Following technical problems (the tendency of biomass to accumulate in the reactor and the corking of the withdrawal cannula), this pump has been replaced by a programmable pump (type Master flex L / S model 77200-60), early in the second series of experiments (*CSTR (b)* Fig. 1). This pump operated in discontinuous mode at the maximum withdrawal rate of 280ml/min. It was scheduled for a 3 minutes period for 2.5 hours. The withdraw of excess liquid occurred rapidly through a larger diameter pipe.

The reactor was equipped with an aeration system (a series of air diffusers for aquarium [4a] and two vacuum pumps Millivac [4b]) used to send air into the culture medium and to ensure a perfect mixing within the bioreactor. For the series of experiments *SE2*, the bioreactor was also equipped with a pH control system (a pump [5a] allowed a NaOH solution [5b] with a concentration of 5% to circulate in the system, a pH probe [5c] was immersed in the reactor and was connected to a pH controller [5b]). Finally, oxygen and temperature were followed along the experiments using sensors ([6a] & [6b]) allowing on-line measurements. All the measured variables were stored in a computer [7] thanks to the Odin-Silex acquisition and control system[1]. Specific conditions for all experiments are reported in Table 1.

Table 1: Experimental conditions and reactor monitoring

	SE1	*SE2*
Reactor	Continuous	Continuous
Substrate concentration S_{in}	1, 2 and 4 g/L	8, 6, 4, 2 and 1 g/L
Initial biomass concentration and dilution	Low concentration (2.58 g/L) obtained after a four-fold dilution with water	High concentration (11.93 g/L), obtained without any dilution after elimination of supernatant
Sludge characteristics	Bad settling	Good settling
HRT	24 h	24 h
Sampling place	Outlet of the reactor	Directly in the reactor
Adding of NaHCO3 in S_{in}	-	Only for high loads: S_{in} = 8, 6 and 4 g/L
pH control system	-	
Other measurements	Microbial fingerprinting Microscopic observation	Microbial fingerprinting Granulometry monitoring

2.2. Analytic monitoring

Various variables were measured daily (excepting the weekends) during the experiments. The pH was measured with a pH-meter (brand of probe: Mettler Toledo transmitter 2100e + probe 405 DPAS-

[1] https://team.inria.fr/biocore/fr/software/odin/

SC-K8S/225). After centrifugation of samples (15 min at 15000 RPM), the supernatant samples were collected and the *COD* measured (micro-method: (kits Hach) spectrophotometer AQUA LYTIC). Biomass samples were collected and the concentrations of suspended solids *SS* and volatile suspended solids *VSS* were determined according to standard methods. In the present study, it is estimated that *SS* are equivalent to *VSS*. In other words, we assumed that the mineral fraction was negligible in such a way *SS* is considered to measure biomass. *COD* was chosen to quantify the substrate concentration. For *SE1*, microscopic observations were carried out by a microscope OLYMPUS DP 80. For *SE2*, LS200 laser granularity was used to determine the floc size distribution *FSD* of the biomass material in the reactor and in the outlet.

For all experiments, a sample from the reactor was put into two screw microtubules of 2ml which were then centrifuged for 10 minutes at full speed using a benchtop centrifuge. The supernatant was then removed and the pellet was stored at - 20 °C. For each experiment at a constant S_{in}, at least 3 samples were selected for molecular biology analyses: one at the starting of experiment, an intermediate or more (according to the duration of the experience) while the system was not yet stabilized and one at the end when the equilibrium is established in the system. To perform a molecular analysis, samples were processed as follows: passing the Cell Lysis and removal of inhibitors, purification (rapid method), DNA extraction (using the QIAamp DNA Mini Kit) and verification with Nano Quant (Micro-plate Reader I-MET-0078 V1), DNA PCR amplification of the V3 region of the 16S rRNA gene (*cf.* Gévaudan et *al.*, 2011) and, finally the analysis of diversity by Single Strand Conformation Polymorphism *SSCP* using the analyzer (3130 Genetic analyzer). To interpret the *SSCP* results, in addition to the *SSCP* profiles obtained for different samples selected, the Simpson indices were computed. These indices were calculated by an algorithm implemented in the software *Statfingerprint*.

2.3. Equilibrium for Monod- and Contois-type kinetics in classical chemostat model

The classical chemostat model is a deterministic set of differential equations allowing to simulate the variations over the time of both substrate and biomass concentrations (denoted *s(t)* and *x(t)*, respectively) in a homogeneous continuous reactor from initial conditions *s(0)*, *x(0)* (*cf.* Harmand *et al.*, 2017). Together with the corresponding experimental setup, a mathematical model has been proposed by both Monod and Novick and Szilard in the fifties (*cf.* Monod, 1950 or Novick and Szilard, 1950) and consists in the following set of equations:

$$\begin{cases} \frac{dx}{dt} = (\mu(\cdot) - D)x \\ \frac{ds}{dt} = -\frac{\mu(\cdot)}{Y}x + (S_{in} - s)D \end{cases} \quad (1)$$

It should be noticed that this model does not include mortality terms. If mortality may play an important role in microbial dynamics when grown in batch mode as in Al-Qodah et *al.* (2007), it can often be neglected when working in continuous mode as long as *D* is large enough. Indeed, at most, mortality is usually considered to be less than 10% of maximum growth in complex environmental microbial ecosystems. Here, since the hydraulic retention time if very short (24h), mortality was neglected.

Depending on the expression of the function $\mu(\cdot)$, the predictions of this model with respect to the steady state of the chemostat considerably vary (*cf.* Harmand et *al.*, 2017). In particular, if $\mu(\cdot)$ depends only on the substrate concentration s, *i.e.* if $\mu(\cdot) = \mu(s)$, the equilibrium of the system (1) is defined as the solution of the following set of equations:

$$\begin{cases} 0 = (\mu(s^*) - D)x^* \\ 0 = -\dfrac{\mu(s^*)}{Y}x^* + (S_{in} - s^*)D \end{cases} \quad (2)$$

The Monod equation *cf.* Monod, 1950 is a substrate-dependent kinetic where the equation relating μ and *s* as is known as follows:

$$\mu(s) = \mu_{max}\frac{s}{s + K_s} \quad (3)$$

where μ_{max} is the maximum specific growth rate and K_s is the half-saturation constant.

Under the assumption that μ is a *monotonously increasing function* of *s*, such that $\mu(0) = 0$ (as, for instance, in the well-known Monod function), and excluding the trivial solution $x^* = 0$ which corresponds to the *washout* of the reactor, we recall two important qualitative results (in the sense they do not depend on model parameters) about the equilibrium of the system (1).

The substrate concentration value at steady state s^* depends only on *D* (providing $D < \mu(S_{in})$). In particular, since μ is a monotonous function, the steady state s^* can be determined uniquely from the equation $s^* = \mu^{-1}(D)$, when this quantity is well defined (*i.e.* $D < \mu_{max}$) and is less that S_{in} (otherwise the washout is the only equilibrium of the system).

From (2), we have then $x^* = Y(S_{in} - s^*) = Y\left(S_{in} - \mu^{-1}(D)\right)$.

Now, consider that $\mu(\cdot)$ depends not only on *s*, but also on *x* (*i.e.* it is *density-dependent*): it is then written as $\mu(\cdot) = \mu(s, x)$. In addition, a very common assumption is that $\mu(s, x)$ is increasing with *s*, but decreasing with *x* (*cf.* for instance Lobry and Harmand, 2006). An example of such kinetics is the well-known Contois function (*cf.* Contois, 1959) where the μ equation can be written in the following form:

$$\mu(s,x) = \mu_{max}\frac{s}{s + K_s x} \quad (4)$$

The computation of the steady state of the system (1) then necessitates solving the following system where the two equations of the system (1) are explicitly coupled by μ through its dependence on both state variables:

$$\begin{cases} 0 = (\mu(s^*,x^*) - D)x^* \\ 0 = -\frac{\mu(s^*,x^*)}{Y}x^* + (S_{in} - s^*)D \end{cases} \quad (5)$$

The following qualitative results can then be established:

- The steady state value of both substrate and biomass concentrations now depends on both the dilution rate *D* and the input substrate concentration S_{in}.
- Since $\mu(s,x)$ is an increasing function of s^* but a decreasing function of *x*, a simple reasoning allows one to establish that both s^* and x^* are increasing functions of S_{in} :

  If we consider the *Contois-type kinetic* (4), x^* will be an increasing function of S_{in} (recall *D* is fixed). At steady state, we have $z^* = \frac{x^*}{Y} + s^* = S_{in}$. If S_{in} increases, the asymptotic value of z^* also increases. At any steady state, one has $\mu(s^*,x^*) = \mu(s^*, Y(S_{in} - s^*)) = D$.

  Differentiating with respect to S_{in}, one obtains: $\frac{\partial\mu}{\partial s}\frac{\partial s^*}{\partial S_{in}} + Y\frac{\partial\mu}{\partial x} - Y\frac{\partial\mu}{\partial x}\frac{\partial s^*}{\partial S_{in}} = 0$.

  As $\frac{\partial\mu}{\partial s} - Y\frac{\partial\mu}{\partial x}$ is a positive number, one can write: $\frac{\partial s^*}{\partial S_{in}} = \frac{-Y\frac{\partial\mu}{\partial x}}{\frac{\partial\mu}{\partial s} - Y\frac{\partial\mu}{\partial x}} > 0$. Thus, when S_{in} increases, either x^* or s^* – or both values – increase and higher S_{in}, higher $x^*$and s^*.

These qualitative properties of the model (1) with respect to its steady state are summarized in Table 2 depending on the mathematical properties of $\mu(\cdot)$.

Table 2: Dependence of the equilibrium with respect to D and Sin for Monod- and Contois-type kinetics

Kinetics	$\frac{\partial\mu}{\partial s}$	$\frac{\partial\mu}{\partial x}$	*Dependence of* s^*	*Dependence of* x^*
Monod-type[2]	+	NC	*D*	S_{in}
Contois-type[3]	+	-	*D* and S_{in}	*D* and S_{in}

These simple qualitative results are at the origin of the present work. As already suggested in the literature, we propose to investigate whether density-dependent growth rate can emerge from high biomass density. This hypothesis originate from the fact that it would rather be the ratio *s*/*x* which

[2]The term "*Monod- type kinetics*" defines any kinetics which is increasing with respect to *s* (*s* being its only argument)
[3]The term "*Contois-type kinetics*" defines any kinetics which is increasing with respect to *s* but which decreases with *x* (*s* and *x* being its only arguments)

conditions growth rate instead of the absolute value of available resource only (*i.e. s*), *cf.* Arditi and Ginzburg, 2012.

Working with a continuous system operating at equilibrium, we proposed here to perform steady-state experiments at different increasing input substrate concentrations as described above in 2.1. The reasoning is based on the fact that - for a *Contois-like growth rate* - the equilibria in x and s depends both on S_{in} and D while - in the case of a *Monod-like growth rate* - the equilibria in x is only affected by S_{in} and the equilibria in s is only affected by D (*cf.* Table 2). In the actual paper, we propose to vary S_{in} while keeping D constant. Thus, whatever the growth rate is, we will observe increasing values for x^*. In other words, higher is S_{in}, the higher is x^*. If the same equilibrium is observed for s^* for both low and high S_{in}, *i.e.* for low as well as for high biomass concentrations, we will conclude that high biomass densities are not the origin of density-dependent growth rates. On the converse, *i.e.* if S_{in} has a significant influence on s^*, it will be concluded that density-dependence may emerge from high biomass densities.

2.4. Model Identification methods

For the data sets that will be obtained from our experiments, ideally, a single model should be searched for in such a way its predictions at equilibrium with the different substrate concentrations tested are in accordance with all experiments. However, with such an approach, our attempts were not successful. As discussed in next sections, S_{in} had a very important influence on the structure of the microbial ecosystem. As a consequence, it was rather decided to develop one model with its specific parameters for each experiment (*i.e.* as many models as experimental sets).

For the parameter optimization, the function “fmincon” of the MATLAB©software was used in minimizing a mean square criterion J. Finally, the value of the criterion, normalized by the number of measurement points, was used to evaluate the quality of each model. In a first attempt, initial conditions (*i.e.* the initial values of biomass and substrate concentrations at the beginning of each experiment) were considered as unknowns. However, proceeding that way the number of parameters to be identified was increased, leading to very high uncertainties in the identified parameters. It was thus decided to consider the first measurements of each experiment as known initial conditions, reducing thus the number of parameters to be identified. In total, five optimizations were performed corresponding to the five series of data points. For each optimization, the practical identifiability of models (capacity of obtaining a unique set of optimized parameters given the structure of the model and the data set) was assessed by comparing the results obtained for different sets of initial conditions for the parameters. In addition, to guarantee the qualitative properties of candidate models to hold

(*i.e.* the monotony of growth rate functions), the parameters were constrained to be positive.

3. RESULTS AND DISCUSSION

3.1. Raw data analysis and yield determination

The data sets *SE1* and *SE2* are plotted in Figures 2 & 3 and the equilibrium values for each set of experiment and for each S_{in} are presented in Table 3.

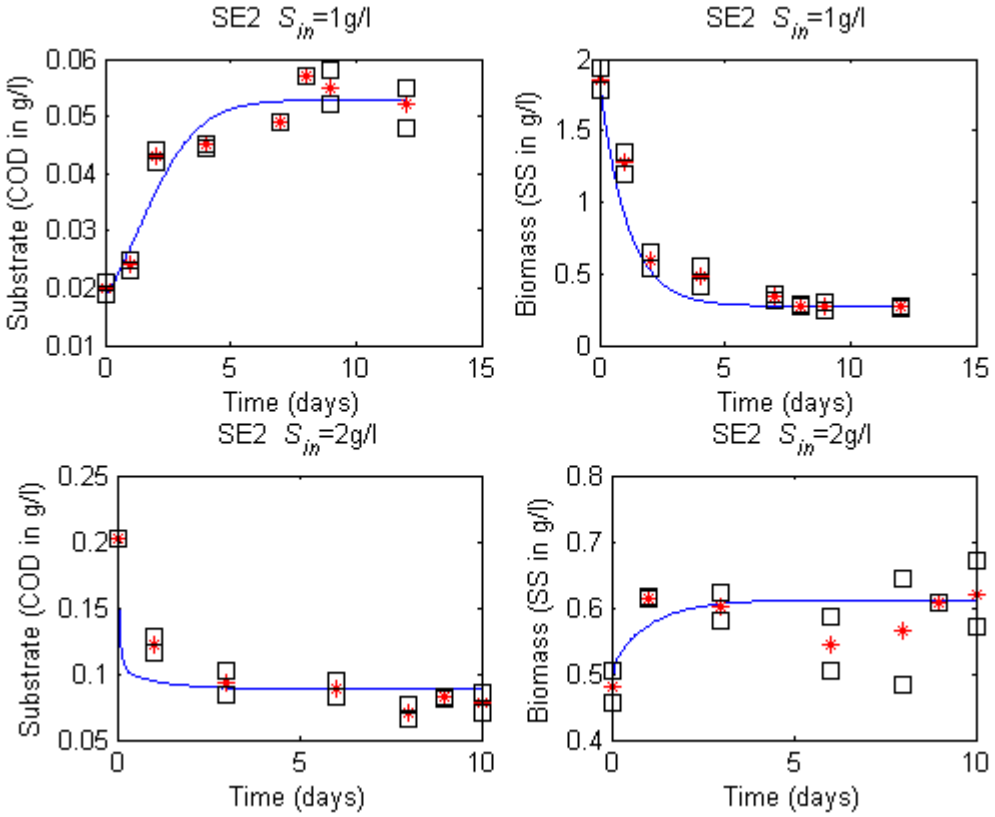

Figure 2: SE1 data sets compared to the model prediction (continuous blue line), (*) is the mean of (□) duplicate measurements of substrate (COD in g/L) and biomass (SS in g/L) in the culture medium under substrate limitation conditions

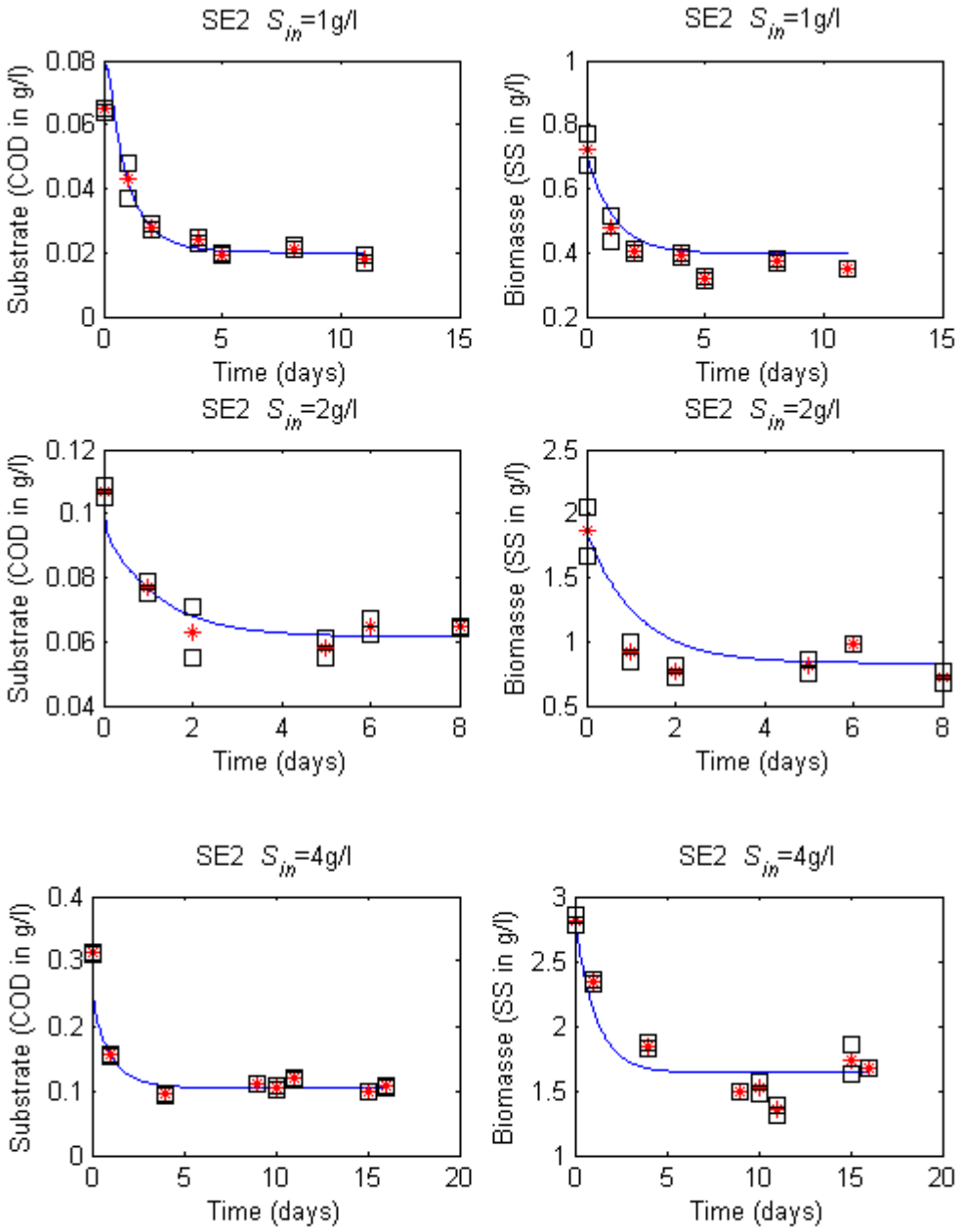

Figure 3: SE2 data sets compared to the model prediction *(continuous blue line), (*) is the mean of (□) duplicate measurements of substrate (COD in g/L) and biomass (SS in g/L) in the culture medium under substrate limitation conditions*

Table 3: Equilibrium values for SE1 and SE2

	SE1		*SE2*		
S_{in} *(g/L)*	0.92	1.95	3.93	2.00	0.95
x^* *(g/L)*	0.27	0.61	1.71	0.84	0.35
s^* *(g/L O_2)*	0.06	0.08	0.10	0.06	0.02
$\lvert\Delta s^*\rvert$ *(g/L)*	0.03		0.04		0.04
s^*/x^*	0.20	0.13	0.06	0.07	0.06
$\lvert\Delta(s^*/x^*)\rvert$	0.07		0.01		0.02

We observe from Table 3 that equilibrium values for the substrate are different for all experiments. In addition, all s^*/x^* ratios at equilibrium are also different. In other words, following the theoretical qualitative results recalled in the Material & Methods section, neither a pure *Monod-type* nor a pure *Contois-type kinetics* can explain the data. However, one may also notice that the differences between substrate equilibrium are smaller within *SE1* conditions than within *SE2* (0.025 compared to 0.040 or 0.042). Differences between equilibrium ratios s^*/x^* are more important for *SE1* than for *SE2* supporting the fact that kinetics followed by the ecosystem during *SE1* is closer from a resource-dependent kinetics while it is closer from a density-dependent kinetics during *SE2*.

Conversion yields can be computed from Table 3 data and are reported in Table 4. A first observation is that the yield is smaller for *SE1* than for *SE2*. A second observation is that it is correlated to S_{in}: higher S_{in} higher the yield.

Table 4: Conversion yields

Data set	*SE1*		*SE2*			
S_{in} *(g/L)*	0.92	1.95	7.56	3.93	2.00	0.95
Y (g/g)*	0.32	0.33	0.46	0.46	0.43	0.38
*Y** by series (g/g)*	0.32		0.43			

** equal to $x^*/(S_{in} - s^*)$.*
*** equal the slope of the plot between x^* versus $(S_{in} - s^*)$.*

It is usually considered that 0.6 is the maximum yield for aerobic processes. For wastewater treatment processes, a net yield (including mortality) of 0.3 to 0.5 are commonly used (Grady, 1999). Obviously, the values for the yield identified here are within this range.

3.2. Microscopic observations

Microscopic observations were realized for *SE1* with increasing substrate step-loads. After the dilution of sludge and before beginning feeding, dense, well enough structured and broken flocs are observed. These flocs of bacteria are associated with several filamentous with few free bacteria found in a clear and clean interstitial liquid (*cf.* Figure 4, MO-1). After 3 days of continuous feeding with the solution of wine at input concentration S_{in} = 1 g/L, flocs became denser and are associated to some filaments (*cf.* Figure 4, *MO-2*). By increasing the feeding concentration to 2 g/L, the observed flocs are denser and denser and we note the presence of several free bacteria which soak in the dark interstitial liquid (*cf.* Figure 4, *MO-3*). According to those observations, we notice that higher S_{in}, denser the flocs.

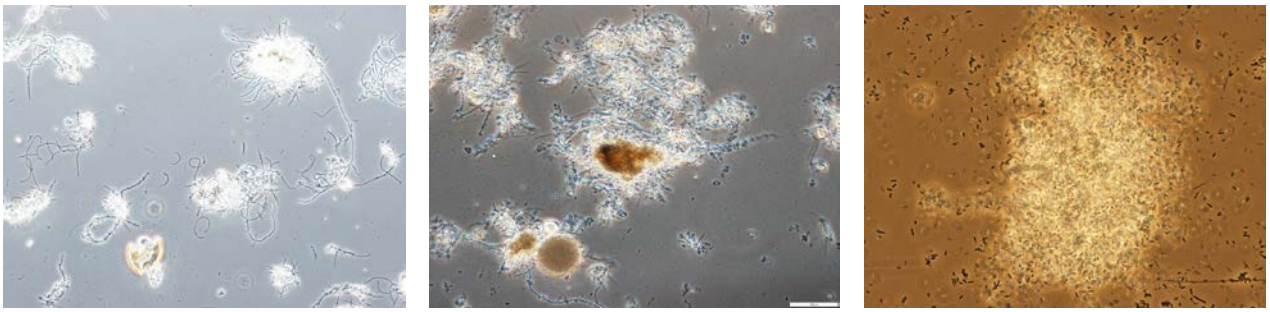

(*MO-1*) Diluted sludge before feeding

(*MO-2*) After 3 days of feeding with S_{in} = 1 g /l

(*MO-3*) At the equilibrium state of S_{in} = 2 g/L

Figure 4 : Microscopic observations

3.3. Floc size distribution

The analyses of the grading distribution of the biomass were realized only for *SE2* with decreasing substrate step-loads. Successive *FSD* 1, 2, 3 and 4 (*cf.* Figure 5) represent the results of the size grading in the reactor (in continuous lines) and at the outlet (dashed lines) for the different loads S_{in} = 8, 4, 2 and 1g/L, respectively. For all the loads, the *FSD* in the reactor and in its outlet were very similar. A very small proportion of free bacteria of lower size than 10µm is present with S_{in} = 8 g/L and 4 g/L. For S_{in} = 8 g/L, besides the small percentage in volume of bacteria (0.2 %), small flocs of 40 µm (3.7 %) and bigger flocs with sizes between 100 and 200 µm (3.4 %) are present. The *FSD* shows that there is a spatial heterogeneity in the reactor. From *SE2* data available at S_{in} = 4, 2 and 1 g/L, only big flocs are present in the reactor. The observed peak of the *FSD* is more and more "moved towards the right" by reducing the feed concentration S_{in} (for S_{in} = 2 and 1g/L, the mean size of the flocs is greater than 2000 µm). This means that the flocculation is more and more important by lowering the load.

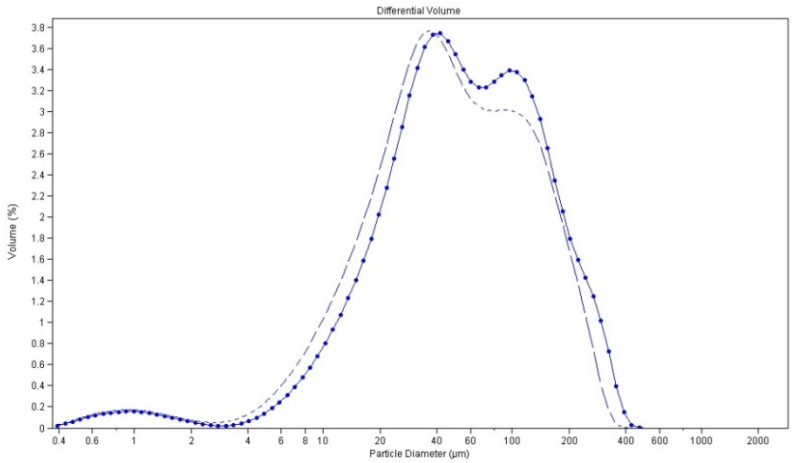

(*FSD*-1) *FSD* at the equilibrium state obtained at S_{in} = 8 g/L

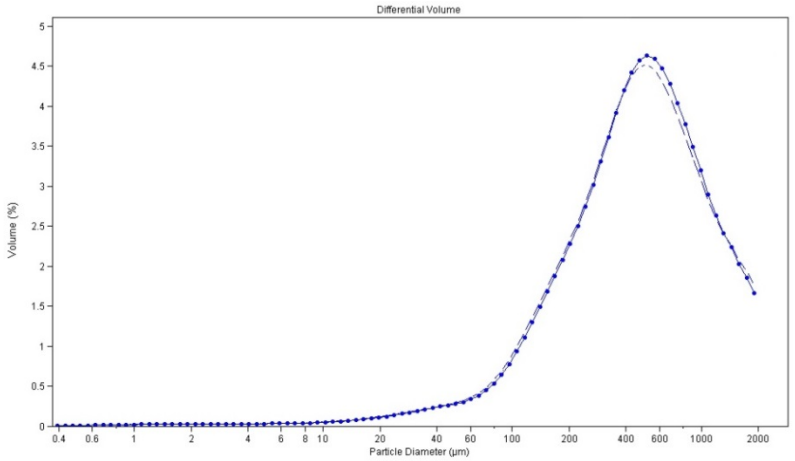

(*FSD*-2) *FSD* at the equilibrium state obtained at S_{in} = 4 g/L

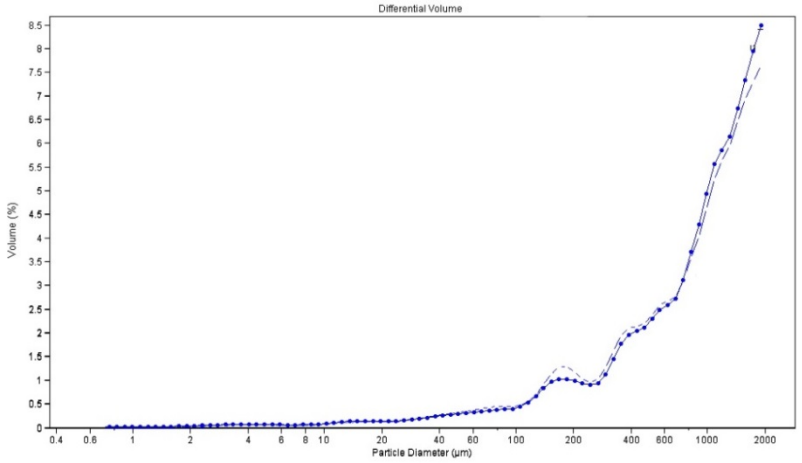

(*FSD*-3) *FSD* at the equilibrium state obtained at S_{in} = 2 g/L

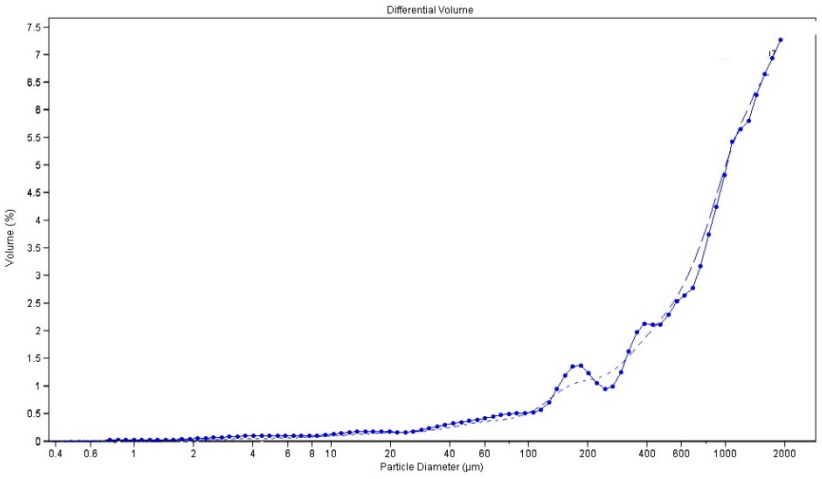

(*FSD*-4) *FSD* at the equilibrium state obtained at S_{in} = 1 g/L

Figure 5: Floc size distribution

3.4. Microbial communities' structure and diversity

The result of the molecular biology obtained by *SSCP* allows us to monitor the microbial structural evolution of the ecosystem. The question of interest here is: does this structure depend on the levels of the input substrate concentration?

Table 5 shows that Simpson indices are similar for all samples except for points P01 and P02 (corresponding to initial ecosystems for *SE1* and *SE2*, respectively) that are themselves very similar (*cf.* Figure 6). The number of peaks visible in Figure 6 for P01 and P02 is important, which highlights a high complexity of the initial ecosystems (recall the inoculums is sludge of a wastewater treatment plant).

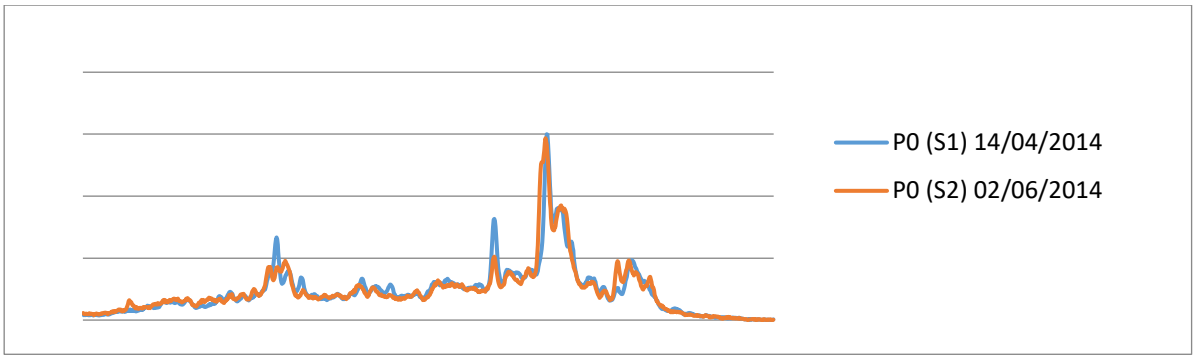

Figure 6: Profiles SSCP of starting points P01 & P02 samples

Table 5: Simpson diversity indices 'SIMPS' and number of the SSCP peaks estimated by Statfingerprint software for position points: P0 (at the starting), inter (before the system stabilization) and end (at the equilibrium)

	S_{in}	Position	Sample	Number of Peaks of the SSCP	- log(SIMPS)	1 - SIMPS
SE1	1 g/L	P0	14-04-14	32	5.03	0.99
		inter	20-04-14	11	2.74	0.94
		end/P0	28-04-14	19	3.40	0.97
	2 g/L	inter	06-05-14	28	4.48	0.99
		end/P0	16-05-14	9	1.97	0.86
	4 g/L	inter	22-05-14	17	3.60	0.97
		end/P0	28-05-14	20	3.44	0.97
SE2	8 g/L	P0	02-06-14	38	6.04	1.00
		inter	06-06-14	16	3.35	0.96
		end/P0	16-06-14	16	3.16	0.96
	6 g/L	inter	20-06-14	10	2.34	0.90
		end	26-06-14	17	2.24	0.89
	4 g/L	P0	27-06-14	16	2.33	0.90
		inter	30-06-14	21	3.18	0.96
		inter	04-07-14	20	2.97	0.95
		inter	11-07-14	21	2.01	0.87
		inter	17-07-14	7	1.92	0.85
		end/P0	23-07-14	16	2.10	0.88
	2 g/L	inter	28-07-14	16	2.98	0.95
		end/P0	31-07-14	23	3.32	0.96
	1 g/L	inter	02-08-14	18	2.03	0.87
		inter	06-08-14	34	3.85	0.98
		inter	11-08-14	25	3.64	0.97
		end	13-08-14	38	4.03	0.98

The Simpson indices of these two initial points (*cf.* Table 5) are greater than all the others. Thus we observe a reduction of the diversity, what is in compliance with what can be expected in a chemostat in which the slowest species should be washed out if they evolve freely in the system. Observing the *SSCP* profiles, we notice that the transitions are quite fast after input concentration changes. It is why we concentrate on large trends and only variations between initial and final points are analysed for each input substrate concentration.

If we suppose that each peak of an *SSCP* profile represents one species, the most important peaks represent corresponding dominant species. It is noticed that major operational taxonomic units (OTU) are never the same at the beginning and at the end of an experiment. Although the initial points P01 and P02 are very similar (*cf.* Figure 6), we notice also that dominant species for identical input

substrate concentrations S_{in} (S_{in} = 1, 2, 4 g/L), whether it is by increasing or by decreasing the load, are different (*cf.* Figure 7). In other words, community structures are not resilient. Each input substrate concentration seems to select a different microbial community. The structure of communities in the chemostat was dynamic. This can be explained by the fact that we work in open conditions. Since the reactor is not sterile, it is permanently inoculated and possibly invaded by bacterial communities present in the liquid feed and/or in the aeration. Furthermore, the presence of predators and virus in the system, even if abiotic and biotic parameters are constant, can also explain dynamics in the ecosystem. The quite high diversity which maintains in the reactor can be explained by the structuration of the microbial community into flocs that become larger and larger over the time as shown by *FSD*.

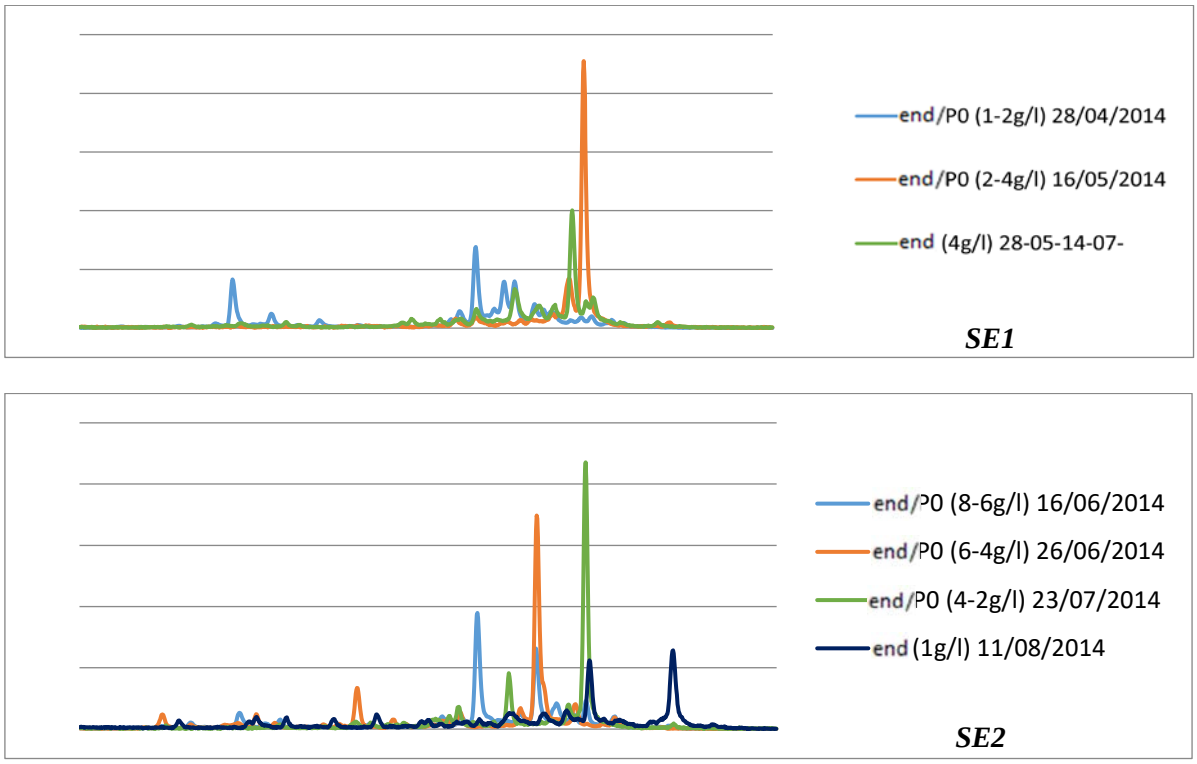

Figure 7: SSCP of the final points for all the experiments

By analyzing the results of molecular biology, several questions arise in terms of modelling. It is useful to know *i)* if populations that are different for each input substrate concentration can be compared and *ii)* if it is necessary to look for a global model for aerobic microbial ecosystems that have the same history but do not have the same behaviour at a given input concentration. In a first attempt, we tried to model, predict and compare what models can explain the experimental data. These trials led to results that are confirmed by molecular biology analyses: the concentration of S_{in} strongly affects the structure of the population at all loads. In particular, a very limited number of species seems to take over but these are never the same. In other terms, the microbial ecosystem obtained

over a given load is very different than that obtained for another load. This result fully justifies modelling experiments separately one from each other. In other words, a different model is used for each S_{in} concentration. Since species are not the same at each load, a single model for all data is insufficient. The fact that communities change according to each input substrate concentration, justifies the fact that the parameters of the models must be re-identified. This is the approach we have adopted to get the identification results for both *SE1* and *SE2* and the results of which are presented in the next section.

3.5. Modelling results - confrontation to data

To formalize our argument, a classical modelling approach was followed. It consisted in identifying the parameters of a number of resource- and density-dependent kinetics models using the data generated by the experiments performed in a continuous biological reactor. From a mathematical point of view, the candidate growth rate function in the model was increasing with respect to the substrate concentration and decreasing with respect to the biomass. Since we worked with a highly biodegradable substrate, the measured substrate concentrations were very low. In such a situation, it is well known that the parameters of the Monod model (3) are not identifiable (only the rate at the origin, that is the ratio of μ_{max} over K_s Monod parameters, can be identified (*cf.* for instance Dochain and Vanrolleghem, 2001)). Thus, we propose to modify the expressions of the candidate growth rates model, introducing a new growth function parameterized as follows:

$$\mu(s,x) = \mu_0 \frac{s}{x^{\alpha}} \tag{6}$$

where α, is a positive parameter that "measures" the density dependence, and in particular, *s* does not appear anymore at the denominator. From now on, we will refer to this model as model (6). Notice that the idea followed here was not to precisely identify the parameters of a given growth rate, but rather to establish qualitatively the resource or the density-dependent character of the kinetics. It also means that the identified values cannot be easily interpreted: it is the reason why we did not name the parameters μ_{max} nor K_s but rather used the notations μ_0 and α. The model with $\alpha = 0$ can be seen as the approximation of the Monod model (3) with $\mu_0 = \mu_{max}/ K_s$ as long as the concentration of substrate is low (typically lower than K_s), and with $\alpha = 1$ as an approximation of the Contois model (4). Therefore, this new model tries to reconcile both model choices in a single model.

As already said, the model variables are *COD* for *s* and *SS* for *x*. For simplicity, the temperature was considered as constant while the oxygen concentration was supposed to be non-limiting.

To identify the model parameters, we can proceed as follows: solving the system (5) (section 2.3.)

and according to model (6) at the steady state, one has

$$\mu_0 \frac{S_{in} - x/Y}{x^\alpha} = D$$

$$\frac{\mu_0}{Y^\alpha} \frac{s}{(S_{in} - s)^\alpha} = D$$

which implies $log\, s = \alpha(log\, x - log(S_{in} - s)) - \alpha log Y$.

Therefore, if one plots, $log(S_{in} - x/Y)) - log\, s$ as a function of $log\, x - log(S_{in} - s)$, a simple linear regression provides the coefficient α. Unfortunately, within these experiments, we got too few data (5 steady states only) to use this approach.

Based on the identification procedure detailed in section 2.4, the whole dynamics over the time was used (from a given initial condition until the end of the experiment, *i.e.* when the system is supposed to have reached almost a steady state). The estimated parameters of model (6) are given in Table 6 and 7 for *SE1* and *SE2*, respectively. The simulations of the proposed models are compared to the experimental data of *SE1* and *SE2* in Figures 2 and 3, respectively.

Table 6: Identification results for SE1

S_{in} (g/L)	*Parameters/Criterion*	*Model (6)*	*Standard deviation*
1	μ_0	10.47	± 1.59
	α	0.41	± 0.13
	J	0.18	-
2	μ_0	10.46	± 2.37
	α	0	± 0.42
	J	0.05	-

Table 7: Identification results for SE2

S_{in} (g/L)	Parameters/Criterion	Model (6)	Standard deviation
1	μ_0	1.42	±0.29
	α	3.92	±0.25
	J	0.03	-
2	μ_0	11.75	±0.67
	α	1.54	±0.35
	J	0.25	-
4	μ_0	29.90	±15.79
	α	2.35	±0.98
	J	0.36	-

3.6. Discussion of modelling results

We first observe that except for S_{in} = 2 g/L of *SE1*, all models exhibit a - more or less - strong density-dependence. This can be correlated with the complexity of biomass instead of its density. Indeed, for *SE1*, recall that we performed experiments in series: the final state of the experiment realized with S_{in} = 1 g/L is the initial conditions for the experiment realized with S_{in} = 2 g/L. Clearly, the structure of the community between the beginning of the first experiment (characterized by a quite high density of filamentous bacteria) and the end of the second experiment has simplified very much. This result could be summarized as follows: as long as the biomass concentration is low, simpler the structure of the community, more important the resource-dependency. For *SE2*, recall that these results have been obtained sequentially in realizing the experiments with decreasing values of S_{in} from 4 g/L to 1 g/L, the first observation is that we obtained increasing values for μ_0. In addition, models for all loads exhibit density-dependence. The differences observed on the values of μ_0 can again be explained by the structure of the ecosystem which is significantly simpler and less structured (with smaller flocs) at S_{in}=1 g/L than at S_{in}=4 g/L which actually supports our claim about density-dependence (refer to the monitoring of granulometry during experiments presented in floc size distribution section**.** The second important point to be underlined is that, except for *SE1* when S_{in}=2 g/L, α is never null even if we subtract the corresponding standard deviation (*cf.* Table 7). This fact confirms the density-dependent character of the growth rate as soon as the biomass is structured into flocs or its density becomes high enough.

4. CONCLUSION AND PERSPECTIVES

In this paper, we analyzed the results of experiments realized in a chemostat to study the growth rate properties of a complex microbial ecosystem. To do so, we relied on experimental data of two series of experiments named *SE1* and *SE2*. The main characteristics of the chemostat were monitored over the experiments, including variables such as the biomass and substrate density, microscopic observations, the structure of the bacterial community and the granulometry of flocs. In addition, a

modeling approach was used considering separate identifications for data obtained at the different input substrate concentrations considered. The analysis of steady-state raw data allowed us to show that biomasses growth rates were not following neither *pure* Monod nor Contois laws. The new model we propose presents a parameter α that measures the strength of density dependency. The growth kinetics obtained for *SE1* data sets presented a weak density dependent effect (low $\alpha \leq 0.41 < 1$) both at low substrate concentration and in the presence of flocs and filaments. Then for $S_{in} = 2$ g/L, being simpler in structure and low in biomass concentration, the effect that emerged is rather resource-dependent ($\alpha = 0$). This fact was confirmed under conditions where biomasses are mainly formed by a lot of free bacteria and some small flocs. It is suspected that the substrate-dependent relationship that was expected to appear with applying low substrate concentration in *SE2* as in *SE1* has been hidden by a high structuration of the biomass into flocs. *SE2* data sets characterized also with greater biomass concentrations conditions than in *SE1*, was best fitted by models with density-effect ($\alpha > 1$) emphasizing high density dependence relations and confirmed by flocculation of biomass. This finding is based on the idea discussed in the literature that spatial structuration of biomass (here via flocculation) justifies the consideration of density-dependent growth model in the chemostat, as it was introduced in the field of mathematical ecology (Arditi et Ginzburg, 2012) or engineering of wastewater treatment processes (Harmand and Godon 2007, Lobry and Harmand, 2006).

AKNOWLEDGEMENTS

Authors thank Roger Arditi for fruitful comments in designing the experiments and the discussions we had about the results during the Bernoulli Seminar Series workshop *Microbial ecology and mathematical modelling* (15–19 December 2014), part of the *Role of mathematics and computer science in the ecological theory Program*, July–December 2014, CIB/EPFL, Lausanne, Switzerland. The first author recognises the help of the Ministry of Higher Education of Tunisia for the half-scholarship awarded to her and is gratefully to LABEX NUMEV and ADEME for funding her PhD grant.

REFERENCES

Arditi, R., L. R. Ginzburg (2012) How species interact – Altering the standard view on trophic ecology, Oxford University Press.

Contois, D. E. (1959). Kinetics of bacterial growth: relationship between population density and specific growth rate of continuous cultures. J. Gen. Microbiol. 21: 40-50.

Daigger, G. T. and Grady, C. P. L., Jr. 1977. A model for the bio-oxidation process based on product formation concepts.– Water Res. 11: 1049–1057.

Dochain, D. and P. Vanrolleghem 2001. Dynamical Modelling & Estimation in Wastewater Treatment Processes, IWA publishing 2001, 360 pages.

Elmaleh, S. and Ben Aim, R. 1976. Influence sur la cinétique biochimique de la concentration en carbone organique à l'entrée d'un réacteur développant une polyculture microbienne en mélange parfait. – Water Res. 10: 1005–1009.

Gévaudan G, Hamelin J, Dabert P, Godon J-J, Bernet N. (2012) Homogeneity and synchronous dynamics of microbial communities in particulate biofilms: from major populations to minor groups. Microbes Environ. 2012; 27:142–148.

Grady, C. P. L., Jr., Harlow, L. J. and Riesing, R. R. 1972.Effects of growth rate and influent substrate concentrationon effluent quality from chemostats containing bacteria inpure and mixed culture. – Biotechnol. Bioengineer. 14:391–410.

Grady, C. P. L., Jr. and Williams, D. R. 1975. Effects of influent substrate concentration on the kinetics of natural microbial populations in continuous culture. – Water Res.9: 171–180.

Grady L. C. P.; Glen Jr ;Daigger T et Lim H. C. (1999): Biological wastewater treatment. Second edition. New York. Basel. Marcel Dekker, 1076p.

Hardin, G. (1960). The competitive exclusion principle. Science 131(3409): 1292-1297.

Harmand, J. and J. J. Godon (2007) Density-dependent kinetics models for a simple description of complex phenomena in macroscopic mass-balance modeling of bioreactors, Ecological Modelling, Volume 200, Issues 3-4, 24 January 2007, Pages 393-402.

Harmand, J., C. Lobry, A. Rapaport, T. Sari (2017) Le chémostat: Théorie mathématique de la culture continue de micro-organismes, ISTE Edition, 240 pages.

Jessup, C. M., R. Kassen, et al. (2004). Big questions, small world: microbial model systems in ecology. TRENDS in Ecology and Evolution 19(4): 189-197.

Jost, C. (2000). Predator-prey theory: hidden twins in ecology and microbiology. OIKOS 90(1): 202-208.

Lobry, C. and J. Harmand (2006) A new hypothesis to explain the coexistence of N species in the presence of a single resource, CRAS sérieBiologie, Vol. 329, pp. 40-46.

Lotka, A.J., Analytical Note on Certain Rhythmic Relations in Organic Systems, Proc. Natl. Acad. Sci. U.S., 6, 410–415, (1920)

Monod, J. (1950). La technique de culture continue : Theorie et applications. Ann. Inst. Pasteur, Lille 79: 390-410.

Novick, A. and L. Szilard (1950). Experiments with the chemostat on spontaneous mutations of bacteria. PNAS 36: 708-719.

Volterra, V., Variazioni e fluttuazionidelnumero d'individui in specieanimaliconviventi, Mem. Acad.

Lincei Roma, 2, 31–113, (1926)

Wade, M. J., J. Harmand, B. Benyahia, T. Bouchez, S. Chaillou, B. Cloez, J. J. Godon, B. Moussa Boudjemaa, A. Rapaport, T. Sari, R. Arditi, and C. Lobry, (2016) Perspectives in Mathematical Modelling for Microbial Ecology, Ecological Modelling, Vol. 321, pp. 64–74.

Yoshinori, F. (1963) Kinetics of microbial growth and substrate consumption. J. Theor. et Biol. 5, 171-191.

Z. Al-Qodah, H. Daghstani, Ph. Geopel, W. Lafi, Determination of kinetic parameters of α-amylase producing thermophile Bacillus sphaericus African Journal of Biotechnology Vol. 6(6), pp. 699-706, 19 March, 2007.